Journal of Alloys and Compounds, 185 (1992) 151–162
JALCOM 213

Contribution to the knowledge of the electrochemical properties of actinides in non-aqueous media
II: The reduction of hexavalent uranium in various organic solvents

L. Martinot*, D. Laeckmann, L. Lopes**, T. Materne and V. Muller
Laboratory of Analytical Chemistry and Radiochemistry, B6, University of Liège, Sart-Tilman, B-4000 Liège (Belgium)

(Received December 18, 1991)

Abstract

The electrochemical behaviour of hexavalent uranium is reported in various organic solvents at room temperature and also in hexamethylphosphoramide, dimethylsulphone, sulpholane between 310 and 400 K. The reduction of UO_2^{2+} proceeds in two steps, leading to tetravalent uranium. Depending on the solvent acidity, the tetravalent species is either soluble or precipitates as UO_2(cr). Numerous additional kinetic phenomena are evidenced in all the reactions.

Special attention is paid to the deposition of UO_2(cr) in macroscopic quantities.

1. Introduction

In a previous paper in this journal [1], we reported numerous experimental investigations on the electrochemical reduction of tetravalent uranium in different organic liquids — at both 298 and 400 K — and it appeared that a great deal of information was gained by electrochemical transient techniques. In the present paper, we similarly describe the properties of hexavalent uranium while giving special attention to the electrochemical deposition of uranium dioxide on solid electrodes.

2. Experimental details

$Cs_2UO_2Cl_4$ is used as the feed material in all the solvents; the purification of organic liquids and the measurements of the water content together with the facilities have been described previously [1]. Tetramethylenesulphone ($TMSO_2$) (sulpholane) (purity, 98%; Janssen Pharmaceutica) was distilled under reduced pressure (about 1 mmHg; N_2 atmosphere) in the presence

*Present address: Inter-University Institute for Nuclear Sciences, Brussels, Belgium.
**Present address: University of Aveiro, Aveiro, Portugal.

0925-8388/92/$5.00

of CaH_2. The water content ranged between 12 and 17 ppm depending on the sample.

3. Results

We report the most representative results. The following transient techniques were utilized: cyclic voltammetry (CV); normal pulse polarography; differential pulse polarography (DPP); chronoamperometry (CA); chronopotentiometry (CP). The data will be discussed according to the usual procedures advanced by Bard and Faulkner [2] and also by Nicholson and Shain [3] and already used in the preceding paper [1].

3.1. Molten dimethylsulphone at 400 K

The reduction of UO_2^{2+} in molten dimethylsulphone ($DMSO_2$) was investigated with 5×10^{-3} and 2.5×10^{-2} M $Cs_2UO_2Cl_4$ solutions; LiCl, $LiClO_4$ and Et_4NClO_4 were successively used as the conducting salts.

3.1.1. Cyclic voltammetry

Two waves appear on the cathodic scan and one peak on the reverse anodic scan; the oxidation peak originates from the first cathodic peak current as reported in Fig. 1. The observations denote a two-step reduction of UO_2^{2+}. The first step corresponds to a reversible reaction; the second is completely irreversible as deduced from the lack of a corresponding peak on the reverse sweep.

3.1.1.1. First reduction wave. As already observed for numerous experiments [1], the peak potential E_p shifts towards more cathodic values when the sweep rate v increases, as predicted for irreversible reactions, but the presence of a peak on reversal favours a reversible system. For a reversible behaviour, the ratio i_{pa}/i_{pc} equals unity (i_{pa} is the anodic peak current and i_{pc} the cathodic peak current) regardless of the scan rate. In our experiments we find that i_{pa}/i_{pc} changes from 1.05 to 1.4 when the scan rate varies from 0.05 to 0.5 V s^{-1}. Deviation of i_{pa}/i_{pc} from unity is indicative of kinetic complications in the electrode process.

In this case, the variation in the current function $i_p/v^{1/2}$ with the rate of the voltage scan makes it possible to use the experimental relation to define the complete electrode reaction. This plot for the reduction of UO_2^{2+} appears in Fig. 2. The current function $i_p/v^{1/2}$ decreases regularly as v increases from 0.05 to 0.5 V s^{-1} on both graphite and platinum electrodes. According to the analysis of Nicholson and Shain [3], these experimental features fit the model

$$Z \rightleftharpoons O \tag{1}$$

$$O + ne^- \rightleftharpoons R \tag{2}$$

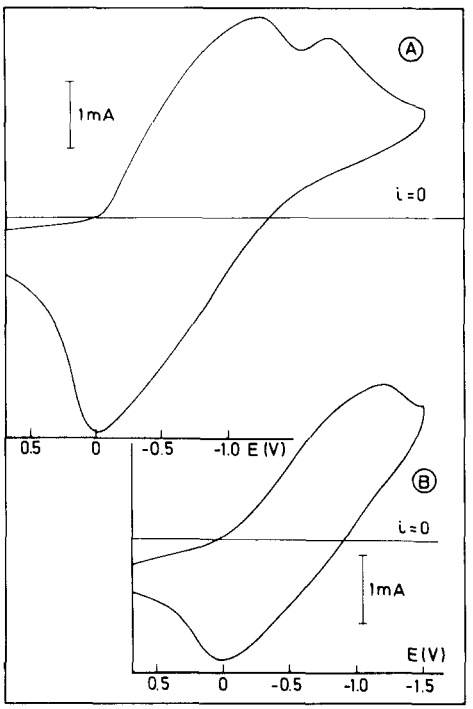

Fig. 1. Voltammetric reduction of $Cs_2UO_2Cl_4$ (2.5×10^{-2} M) in molten $DMSO_2$ at 400 K (platinum cathode): curve A, two reduction waves and one oxidation peak; curve B, the first reduction step.

in which the electroactive species O is produced by a reversible chemical reaction (1) preceding the reversible charge transfer (2); Z may be considered to be a complex species of UO_2^{2+} — with the solvent or with Cl^- ions — which is not electroactive. In the presence of additional kinetic phenomena, the usual electrochemical data cannot be fully interpreted [1]. We consider that UO_2^+ is produced in this first step; the structures of UO_2^{2+} and UO_2^+ are very similar and the presence of a reversible charge transfer reaction may be suggested as in molten salt media [4].

3.1.1.2. Second reduction wave. The peak potential also changes with the sweep rate in the range $0.05 \text{ V s}^{-1} \leqslant v \leqslant 0.2 \text{ V s}^{-1}$ while the formation of a reverse oxidation peak was never evidenced; these facts are consistent with an irreversible reduction of pentavalent uranium probably into a tetravalent species. In the presence of additional kinetic phenomena, the intensity ratio of two consecutive peaks in a stepwise reduction is not a diagnostic criterion [2, 3] to define the number of electrons exchanged in the second reaction. No information is deduced about the so-produced species; we have either a tetravalent ion U(IV) or a solid compound UO_2(cr).

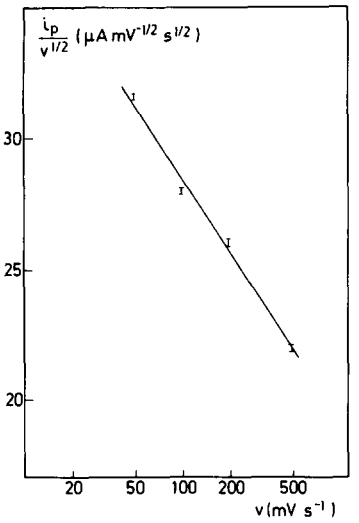

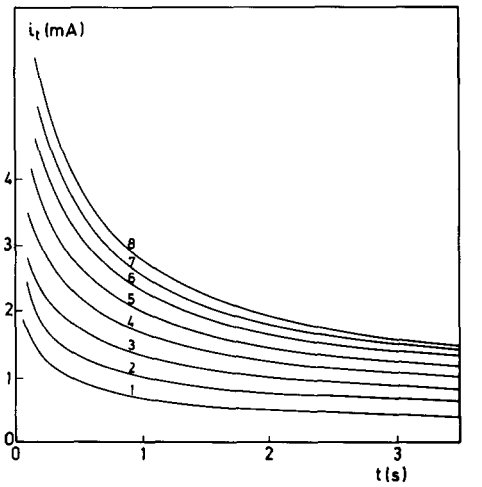

Fig. 2. Plots of the ratio $i_p/v^{1/2}$ against v for the reduction $UO_2^{2+} + e^- \rightarrow UO_2^+$ in $DMSO_2$ at 400 K (graphite cathode; $[Cs_2UO_2Cl_4] = 2.5 \times 10^{-2}$ M).

Fig. 3. Plots of the chronoamperometric current $i = f(t)$ against the time for the reduction $UO_2^{2+} + e^- \rightarrow UO_2^+$ in $DMSO_2$ at 400 K (platinum cathode; $[Cs_2UO_2Cl_4] = 5 \times 10^{-3}$ M) for various potentials against the platinum quasi-reference: curve 1, −500 mV; curve 2, −600 mV; curve 3, −700 mV; curve 4, −800 mV; curve 5, −900 mV; curve 6, −1000 mV; curve 7, −1100 mV; curve 8, −1200 mV.

3.1.2. Chronoamperometry

This technique gives diagnostic criteria that complement the results obtained with CV experiments [1].

3.1.2.1. First reduction wave. For each applied potential stepping from 0.00 V (*i.e.* the foot of the CV wave) to a more cathodic value, we note a continuous decrease in the current i with the time t of electrolysis as illustrated in Fig. 3. Neither the Cottrell law that predicts a linear variation of i with $t^{-1/2}$ for a reversible reaction [2] nor the linear variation in i with $t^{1/2}$ that holds for irreversible reactions [5] is observed except at very low overvoltages; in this latter case, by extrapolating the $i = f(t^{1/2})$ values to zero time, we obtain the k_f values according to

$$k_f = i(0)/nFSC \qquad (3)$$

where $i(0)$ is the extrapolated current for $t = 0$ [5] and S (cm^2) the indicator electrode area. For small overvoltages $E_c = -0.5$ V and $E_c = -0.6$ V, we obtain $k_f \approx 2.7 \times 10^{-3}$ cm s^{-1} and $k_f \approx 4.4\ 10^{-3}$ cm s^{-1} respectively. When comparing k_f with the values obtained by similar calculations in $DMSO_2$ at the same temperature, one can say that the tendency to reversibility of the system UO_2^{2+}–UO_2^+ is greater than that of the system U^{4+}–U^{3+} for which we reported 1.7×10^{-5} cm s$^{-1} \leqslant k_f \leqslant 4.3 \times 10^{-5}$ cm s^{-1} [1].

3.1.2.3. Second reduction wave. The $i=f(t)$ curves are not reproducible but a continuous decrease in the current is observed; the shape of the $i=f(t)$ curves is never distorted. This technique does not allow one to obtain information about the tetravalent species.

3.1.3. Controlled potential electrolysis

A solution of $Cs_2UO_2Cl_4$ (about 4×10^{-2} M) has been reduced with a cathodic potential fixed at -2.8 V. After 12 h of electrolysis (120 C), the yellow colour of the solution had turned to light green which is characteristic of tetravalent uranium introduced in $DMSO_2$ as Cs_2UCl_6 or UCl_4 [1]. The presence of U(IV) has been evidenced by CV measurements. The electrochemical reduction of UO_2^{2+} gives soluble tetravalent uranium while UO_2(cr) originates from the same reaction in molten chlorides [4]. In $DMSO_2$, the UO_2^{2+} ion loses oxygen, indicating that the solvent interferes with the electrode process. Taking into consideration the fact that $DMSO_2$ is a weak acid of approximate pK_a 28.5 [1], we propose the following mechanism:

$$UO_2^{2+} + e^- \rightleftharpoons UO_2^+$$

with

$$UO_2^+ + e^- + 4\ CH_3SO_2CH_3 \longrightarrow U^{4+} + 2\ H_2O(g) + 4[CH_3SO_2CH_2]^-$$

or

$$UO_2^+ + e^- + CH_3SO_2CH_3 \longrightarrow UO_2H^+ + [CH_3SO_2CH_2]^-$$

$$UO_2H^+ + 3\ CH_3SO_2CH_3 \longrightarrow U^{4+} + 2\ H_2O(g) + 3[CH_3SO_2CH_2]^-$$

where UO_2H^+ is the intermediate species evidenced in aqueous solution in the reduction UO_2^{2+}–U^{4+}.

This mechanism is in agreement with the absence of a reverse oxidation peak for the second step in CV experiments (see Section 3.1); electrochemical oxidation of U(IV) could not be achieved in any of our earlier experiments [1].

3.2. Molten tetramethylenesulphone at 400 K

Similar experiments were carried out with $Cs_2UO_2Cl_4$ between 310 and 400 K. $TMSO_2$ ($C_4H_8SO_2$) is a very weak acid ($pK_a \approx 33$) which is more inert than $DMSO_2$.

3.2.1. Cyclic voltammetry

The electrochemical reduction of the uranyl ion proceeds in two steps at both 310 and 400 K. A reverse oxidation peak corresponding to the first step clearly appears at 400 K but is not present at 310 K. The oxidation peak on reversal — corresponding to the second reduction step — exists at both 310 and 400 K. At least at 400 K the tendency to reversibility of the system is greater in $TMSO_2$; additional kinetic phenomena are also ascertained for the two waves but the theoretical models discussed by Nicholson

and Shain [3] do not give proper account for our experimental results. DPP supports the CV results.

3.2.2. Chronoamperometry

3.2.2.1. First reduction wave. The CA investigation indicates that the best fit for the $i=f(t)$ plots corresponds to an irreversible reaction for small cathodic overvoltages. Equation (3) gives $k_f \approx 9 \times 10^{-6}$ cm s^{-1} for $E_c = -0.6$ V at 310 K.

3.2.2.2. Second reduction wave. The network of $i=f(t)$ curves becomes irregular when the cathodic potentials go beyond -1.75 V as illustrated in Fig. 4; a smooth increase in the current with time appears between 1.5 and 3 s. This signifies that the cathodic surface increases as the electrochemical reaction proceeds; the phenomenon is encountered upon uneven covering of the electrode surface by a solid deposit (nucleation). In $TMSO_2$, the deposition of UO_2(cr) would cause nucleation in the early steps of the deposition.

3.2.3. Controlled potential electrolysis

The electrolysis was carried out with a cathodic potential (platinum electrode) fixed at -2.5 V *vs.* the quasi-reference. UO_2(cr) is deposited in a crust of black powdery material originating from the conducting salt (LiCl) and from the solvent decomposition products. The faradaic yield is about 52%; no other uranium oxide (U_3O_8, U_4O_9 or UO_3) was found in the deposit.

It becomes evident that, in $TMSO_2$, hexavalent uranium is reduced in two steps: $UO_2^{2+} \rightarrow UO_2^{+} \rightarrow UO_2$(cr). The solvent is completely inert and the mechanism is similar to that observed in molten (Li, K)Cl but the current yield is lower [4].

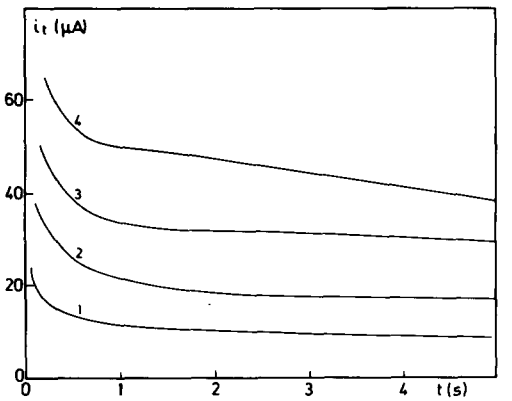

Fig. 4. Plots of the chronoamperometric current $i=f(t)$ against the time for the reduction $UO_2^{+} + e^{-} \rightarrow UO_2$(cr) in $TMSO_2$ at 310 K (platinum cathode; $[Cs_2UO_2Cl_4] = 2.5 \times 10^{-2}$ M] for various potentials against the platinum quasi-reference; curve 1, -1600 mV; curve 2, -1750 mV; curve 3, -1850 mV; curve 4, -1900 mV.

3.3. Ethylene glycol dimethylether

Experiments in ethylene glycol dimethylether (DME) were carried out for $[UO_2^{2+}] = 5 \times 10^{-3}$ M and 2.5×10^{-2} M in the presence of 0.3 M $LiClO_4$; this increased concentration of the conducting salt is required to dissolve the uranyl salt completely.

3.3.1. Cyclic voltammetry

Two waves are identified during the cathodic scan; the first ($E_p = -0.43$ V at 0.05 V s^{-1}) is well defined but the second is poorly shaped and spreads between about -2.2 and about -2.8 V on both graphite and platinum cathodes. The shape of the curve on reversal depends on the concentration of the electroactive species and on the nature of the cathode; a well-defined reversal peak corresponding to the first reduction step appears on platinum for $[UO_2^{2+}] = 2.5 \times 10^{-2}$ M. The complete analysis of the first reduction wave leads to the conclusion that coupled chemical reactions are the causes of the kinetic phenomena.

When the direction of the scan is reversed before the solvent reduction, a characteristic cross-over is observed which indicates the presence of an intense nucleation process [6] due to the deposition of uranium dioxide: $UO_2^{2+} \rightarrow UO_2^{+} \rightarrow UO_2(cr)$.

3.3.2. Chronoamperometry

The departure from complete reversibility of the first wave is confirmed by this technique. According to eqn. (3), we calculate for $[UO_2^{2+}] = 2.5 \times 10^{-2}$ M and -0.30 V $\leqslant E_c \leqslant 0.35$ V, $k_f \approx 1.1 \times 10^{-5}$ cm s^{-1} on both platinum and graphite electrodes. The $i(t) = f(t)$ curves corresponding to the second wave exhibit a rising part when the time exceeds 0.5 s and when the cathodic potentials lie between -2.70 and -3.40 V. A typical curve is reported in Fig. 5.

The nucleation phenomenon identified in a qualitative way from CV experiments may be fully described by the potentiostatic current transients. The current–time relationship for the growth of N crystallites appearing instantaneously is given by

$$i(t) = nF\pi(2DC)^{3/2}M^{1/2}Nt^{1/2}d^{-1/2} \tag{4}$$

where nF is the molar charge of the electroactive species, D its diffusion coefficient, C (mol cm^{-3}) its concentration, M its molecular weight and d its density. In these conditions, a linear dependence of $i(t)$ on $t^{1/2}$ is observed for the rising part of the curve reported in Fig. 5. This condition of arrested nucleation differs from the progressive nucleation where new nuclei are formed continuously and which is described by the equations

$$i(t) = 0.66nF\pi AN_\infty(2DC^{3/2})M^{1/2}t^{3/2}d^{-1/2} \tag{5}$$

$$N(t) = N_\infty[1 - \exp(-AN_\infty t)] \tag{6}$$

where N_∞ is the maximum number of nuclei obtainable under the prevailing conditions and A is the steady state nucleation rate constant per site [6].

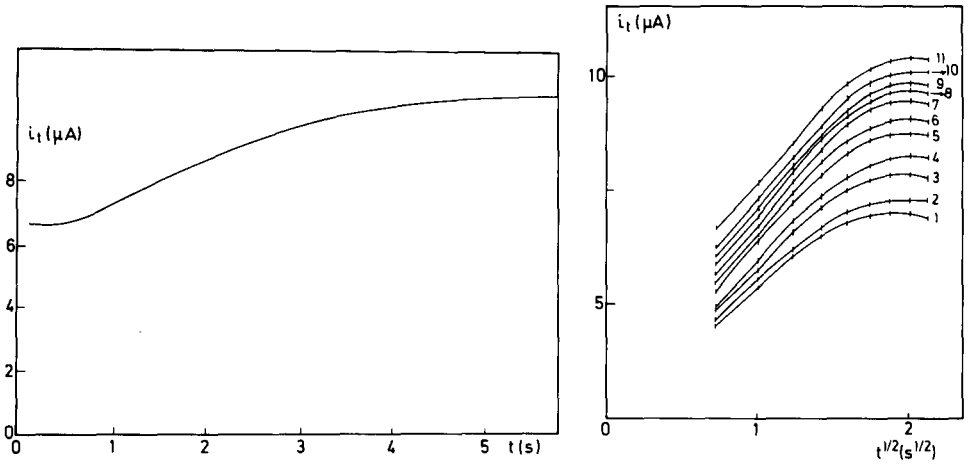

Fig. 5. A typical plot of the increase of the chronoamperometric current $i(t)$ against the time for the reduction $UO_2^{+} + e^{-} \rightarrow UO_2(cr)$ in DME at 298 K (graphite cathode; $[Cs_2UO_2Cl_4] = 2.5 \times 10^{-2}$ M; cathodic potential, −3100 mV against the platinum quasi-reference).

Fig. 6. Plots of the increasing chronoamperometric current $i(t)$ against the square root of the time (conditions: as in Fig. 5): curve 1, −2900 mV; curve 2, −2950 mV; curve 3, −3000 mV; curve 4, −3050 mV; curve 5, −3100 mV; curve 6, −3150 mV; curve 7, −3200 mV; curve 8, −3250 mV; curve 9, −3300 mV; curve 10, −3350 mV; curve 11, −3400 mV.

Equation (5) predicts a linear dependence of $i(t)$ on $t^{3/2}$. The experimental plots reported in Fig. 6 clearly demonstrate an instantaneous nucleation of $UO_2(cr)$ on a vitreous graphite electrode.

3.3.3. Chronopotentiometry

Further information on the nucleation phenomenon has to be collected by CP techniques (galvanostatic transients); a constant current i is applied to the working electrode and the evolution of the potential is recorded. In an unstirred medium, the concentration of the electroactive species at the electrode drops to zero at a certain characteristic time τ called the transition time. At this point, the classical Sand equation holds:

$$\frac{i\tau^{1/2}}{C} = \frac{nFSD^{1/2}\pi^{1/2}}{2} \tag{7}$$

where S is the electrode area. After the transition time, the potential becomes more increasingly negative (in the case of a reduction) until a second reaction takes place. When the investigated reaction leads to the deposition of a solid, the potential–time curve is distorted and an overshoot is sometimes observed. In our experiments on platinum and graphite electrodes ($[UO_2^{2+}] = 2.5 \times 10^{-2}$ M) we always notice an overshoot *vs.* the dynamic potential. Such an overshoot has been called 'superpolarization' by Fleischmann and Thirsk [7] and indicates $UO_2(cr)$ specific growing sites at the electrode surface. The distance l between the growing sites increases at the beginning of the constant current pulse. This is depicted by the formula [7]

$$\eta l = \frac{2\pi V_m \sigma}{nF} \tag{8}$$

where η is the overshoot, V_m (cm^3) the molar volume of the electrodeposited solid and σ (erg cm^{-2}) the surface energy. With $V_m = 25$ cm^3 for UO_2(cr), $\sigma = 500$ erg cm^{-2} [7, 8] and $\eta_{max} = 0.35$ V, we obtain $l \approx 23$ Å for $n = 1$ for the second reduction $UO_2^+ + e^- \rightarrow UO_2$(cr). This formula shows that any increase in l will produce a decrease in η. This order of magnitude is acceptable since Fleischmann and Thirsk [7] have reported $l \approx 30$ Å for silver electrodeposition from aqueous solutions; the values of 45 Å and 28 Å have been recently observed for the nucleation of deposited uranium metal in γ-butyrolactone (4-hydroxylactone butanoïc acid) and in $\beta\beta'$ oxydiproprionitrile (dicyano-diethyl-ether) respectively [9, 10].

The nucleation phenomenon encountered in the electrochemical precipitation of UO_2(cr) is completely described by potentiostatic and galvanostatic transients.

3.3.4. Controlled potential electrolysis

The cathodic potential was fixed at -3.7 V *vs.* the quasi-reference (platinum cathode; $[UO_2^{2+}] = 2.5 \times 10^{-2}$ M). At the end of the experiment, the cathode was covered with a powdery material containing very small quantities of UO_2(cr). In the present case, the powdery material was easily soluble in the solvent and we used a pulsed controlled potential electrolysis instead of the classical continuous electrolysis. The cathodic potential was pulsed from the rest value of -1.4 V to -3.7 V. The potential pulses and the current responses are illustrated in Fig. 7. After 18 h of electrolysis, isolated nodules of UO_2(cr) were deposited on the electrode with a current yield of about 18%. We tentatively explain the deposit as due to the dissolution of the organic decomposition products during the rest periods at -1.4 V under continuous stirring.

3.4. Hexamethylphosphoramide

3.4.1. Transient techniques

The reduction of UO_2^{2+} in hexamethylphosphoramide (HMPA) was investigated for $[UO_2^{2+}] = 1 \times 10^{-2}$ M and 2.5×10^{-2} M at both 298 and

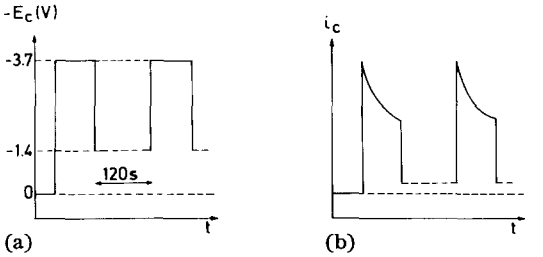

Fig. 7. (a) The potential programme applied at the cathode during the pulse controlled potential electrolysis and (b) the response current in the cell.

400 K to compare these results with the results acquired in molten $TMSO_2$ and $DMSO_2$.

At 298 K, the different techniques evidenced the formation of UO_2(cr) according to the classical two-step reduction $UO_2^{2+} \rightarrow UO_2^{+} \rightarrow UO_2$(cr). The first step is best described by a reversible charge transfer (2) followed by an irreversible chemical reaction (1), *e.g.* a complex rearrangement, of the so-produced pentavalent species. Furthermore, adsorption phenomena were also pointed out. k_f values for this step lie between about 1×10^{-5} and 2×10^{-5} cm s^{-1} for cathodic potentials ranging from -0.620 to -0.650 V (CA measurements). The deposition of UO_2(cr) occurs in the second step but no nucleation phenomenon has been evidenced.

At 400 K, the adsorption phenomena disappeared but the first step ($UO_2^{2+} \rightarrow UO_2^{+}$) has to be considered as a reversible first-order chemical reaction (1) preceding a reversible charge transfer (2). The reason why the mechanism changes with increased temperature is difficult to understand but there could be a modification in the structure of the electroactive species. At 298 K, UO_2^{2+} would be complexed by both the solvent and the chloride anions while, at 400 K, $UO_2Cl_4^{2-}$ would be the predominant species as has been recognized in molten (Li, K)Cl at 673 K [11].

3.4.2. Controlled potential electrolysis

These experiments were achieved at 400 K ($[UO_2^{2+}] \approx 4.8 \times 10^{-2}$ M) with $E_c = -2.45$ V *vs.* the platinum quasi-reference. In all cases a poorly adherent black deposit was noticeable on both the cathode and the bottom of the cell; the colour of the solution had also turned from yellow to brown, suggesting the cathodic decomposition of HMPA. The presence of UO_2(cr) in the precipitates was ascertained by powder X-rays diffraction.

3.5. Dimethylsulphoxide and propylene carbonate

In dimethylsulphoxide (DMSO) and propylene carbonate (PC), hexavalent uranium is reduced in two steps complicated by coupled chemical reactions. In DMSO, the deposition of UO_2(cr) proceeds according to instantaneous nucleation (eqn. (4)) but nucleation no longer holds in PC. We failed to obtain macroscopic quantities of UO_2(cr) in these two solvents because the cathode was covered with an electrochemical deposit of an insulating organic layer.

3.6. Tetrahydrofuran

The dissolution of $Cs_2UO_2Cl_4$ is feasible only in a mixture of tetrahydrofuran (THF) with about 10 wt.% $LiClO_4$; the conductivity reaches 300 Ω cm^{-1}. The voltammetric experiments showed the presence of a well-defined cathodic peak with one weak peak on reversal. The interpretation of this unique cathodic wave has remained impossible. Either the reduction of UO_2^{2+} proceeds in two steps but the second wave vanished because of peculiar values of the kinetic parameters as foretold by Nicholson and Shain [3] or only the first reduction takes place. A two-electron transfer leading to a uranium(IV) soluble species may also be considered.

4. Conclusions

Kinetic factors play an important role in the reduction of hexavalent uranium in all the organic media studied and the investigation of the same reaction by different electrochemical techniques allows only a limited understanding of the phenomena. The appearance of kinetic effects depends on the time window of each investigation method and the values so acquired have to take in account this point of view mainly when numerical values of the kinetic parameters are calculated. Nevertheless, the presence of additional kinetic effects is confirmed in a qualitative way by all the techniques involved. It is evident that CV is the best technique to define a reversible or an irreversible charge transfer coupled with a chemical reaction.

The measurement of the rate constants by CA gives only the order of magnitude according to eqn. (3) for a non-reversible process; k_f depends on the final cathodic potential reached in the potential pulse but some dependence on the concentration is also noticed (Table 1). New experiments are in progress to check the credibility of the CA method with the rotating-disk electrode.

The electrochemical transfer coefficient α — a measure of the symmetry of the energy barrier in the electrode process — may be calculated according to the fundamental equations discussed in a preceding paper [1] or may be deduced from CA experiments after the graphical construction of classical polarograms. The values that were calculated are listed in Table 1; only for DMSO and HMPA do convergent data seem to exist. In these two cases, we shall tentatively conclude that the two methods — CV and CA — are sensitive to the same phenomenon. This may reflect the stability of the UO_2^{2+} cation complexed by the solvents (HMPA or DMSO); only these two solvents form strong complexes because of their P=O or S=O functional group. The different values quoted for α in the two solvents would then correspond to the different sizes of the uranyl complex species related to the different steric volumes of the organic molecules.

TABLE 1

Some kinetic parameters for the reduction $UO_2^{2+} + e^- \rightarrow UO_2^+$

Temperature (K)	Organic medium	k_f (cm s^{-1}) for following $[UO_2^{2+}]$		α obtained by following methods	
		5×10^{-3} M	$2\times5\ 10^{-2}$ M	CV	CA
298	CP	3×10^{-4}	–	0.17 ± 0.02	–
298	DME	1×10^{-6}	1×10^{-5}	0.16 ± 0.08	0.3
298	DMSO	3×10^{-6}	–	0.57 ± 0.06	0.5
298	HMPA	–	1×10^{-5}	0.35 ± 0.02	0.3
310	$TMSO_2$	–	1×10^{-5}	≈0.3	–
400	$DMSO_2$	3×10^{-3}	–	0.25 ± 0.12	–
400	HMPA	–	–	0.32 ± 0.02	–

In some solvents, UO_2(cr) deposits are never obtained even when the formation of the dioxide is predicted by the transient experiments. The simultaneous reduction of the solvent probably shifts the electrodeposition potential and the polarization window becomes too narrow. When $TMSO_2$ and HMPA are involved, macroscopic quantities of UO_2(cr) are gained but, in DME, pulsed electrolysis is required to obtain similar results.

Acknowledgments

We thank the Inter-University Institute for Nuclear Sciences (Brussels) for support of this work and Professor J. Fuger for the useful discussions.

References

1 L. Martinot, D. Laeckmann, T. Materne and W. Müller, *J. Less-Common Met.*, *163* (1990) 185.
2 A. Bard and L. Faulkner, *Electrochemical Methods*, Wiley, New York, 1980.
3 R. Nicholson and I. Shain, *Anal. Chem.*, *36* (4) (1964) 706.
4 L. Martinot and J. Fuger, *J. Less-Common Met.*, *120* (1986) 255.
5 D. Macdonald, *Transient Techniques on Electrochemistry*, Plenum, New York, 1977.
6 G. Gunawardena, G. Hills, I. Montenegro and B. Scharifker, *J. Electroanal. Chem.*, *138* (1982) 225.
7 M. Fleischmann and H. Thirsk, *Electrochim. Acta*, *2* (1960) 22.
8 K. Vetter, *Electrochemical Kinetics*, Academic Press, New York, 1967.
9 C. Michaux, *Thesis*, University of Liège, Belgium, 1991.
10 F. Lebon, *Thesis*, University of Liège, Belgium, 1991.
11 L. Martinot, in A. Freeman and C. Keller (eds.), *Handbook on the Physics and Chemistry of Actinides*, Vol. 6, *Molten Salts Chemistry of Actinides*, North-Holland, Amsterdam, 1991.